Effect of Inoculum Pretreatment on Alcohol Production from Volatile Fatty Acids through an Anaerobic Solventogenic Process

[1,2,3]Gustavo Mockaitis*, [1]Guillaume Bruant, [2]Eugenio Foresti, [2]Marcelo Zaiat, [1]Serge R. Guiot.

[1]Anaerobic Technologies and Bioprocess Control group, Energy, Mining and Environment research center, National Research Council Canada, 6100 Royalmount Avenue, H4P 2R2, Montreal, QC, Canada.

[2]Biological Processes Laboratory, Center for Research, Development and Innovation in Environmental Engineering, São Carlos School of Engineering, University of São Paulo (EESC/USP), Av. João Dagnone, 1100, Santa Angelina, São Carlos, São Paulo 13563-120, Brazil.

[3]Interdisciplinary Research Group on Biotechnology Applied to the Agriculture and the Environment, School of Agricultural Engineering, University of Campinas (GBMA/FEAGRI/UNICAMP), 501 Cândido Rondon Avenue, CEP, 13.083-875, Campinas, SP, Brazil.

(*Corresponding Author, gusmock@unicamp.br)

1 Abstract

Background: Production of alcohols from wastes through biological processes is environmentally and economically interesting, since they can be valorized as drop-in liquid fuels, which have a high market value. Using microbial mixed cultures in such processes is of great interest since it confers more stability, a higher resistance to both toxicity and contamination, and an increased substrate flexibility. However, there is still a lack of fundamental knowledge on such microbial populations used as inoculum in solventogenic processes. This work evaluates the effect of four different physicochemical pretreatments (acidic, thermal, acidic-thermal and thermal-acidic) on an anaerobic inoculum used for alcohols production from volatile fatty acids.

Results: All experiments were conducted in single batches using acetate and butyrate as substrates, at 30°C and with a pressurized headspace of pure H_2 at 2.15 atm (218.2 MPa). Higher productions of both ethanol and butanol were achieved with both thermal and acidic-thermal pretreatments of the inoculum. The highest concentrations of ethanol and butanol produced were respectively of 122 $mg.L^{-1}$ and 97 $mg.L^{-1}$ for the thermal pretreatment (after 710 hours), and of 87 $mg.L^{-1}$ and 143 $mg.L^{-1}$ for the acidic-thermal pretreatment (after 210 hours). Butyrate was consumed and acetate was produced in all assays. A mass balance study indicated that the inoculum provided part of the substrate. Thermodynamic data indicated that a high H_2 partial pressure favored solventogenic metabolic pathways. Finally, sequencing data showed that both thermal and acidic-thermal pretreatments selected mainly the bacterial genera *Pseudomonas*, *Brevundimonas* and *Clostridium*.

Conclusion: The acidic-thermal pretreatment selected a bacterial community more adapted to the conversion of acetate and butyrate into ethanol and butanol, respectively. A higher production of ethanol was achieved with the thermal pretreatment, but at a slower rate. The thermal-acidic pretreatment was unstable, showing a huge variability between replicates. The acidic pretreatment showed the lowest alcohol production, almost negligible as compared to the control assay.

2 Keywords

Solventogenesis, inoculum pretreatment, volatile fatty acids, butanol, ethanol, anaerobic metabolism

3 Background

The constant increase of prices of fossil fuels and the large land requirements for crop cultures targeting ethanol production is forcing the market to consider substitute avenues. Application of bioprocesses with organic residues as raw materials could be an interesting alternative for fuel production. Anaerobic processes can be used to produce alcohols (through solventogenic processes [1]) and volatile fatty acids (VFAs) and hydrogen (H_2) (through acidogenic processes [2]) as fuels. The conversion of any wastes into VFAs and H_2 has an immediate commercial interest. Both propionic and butyric acids are raw materials of great interest, with many applications in various sectors, such as for pharmaceutical and chemical industriesH_2 could also be considered both as a raw material for subsequent processes and as an energy carrier which would feed fuel cells [3].

Although anaerobic acidogenic processes could be an interesting alternative for wastes valorization, downstream processing of the VFAs obtained through those processes, such as bioconversion into their corresponding alcohols using H_2 produced concomitantly, could have an even greater economic interest [4,5]. Ethanol and butanol produced through such processes can be used as drop-in liquid fuels, which have a higher market value per unit of energy. This two-steps approach (acidogenic followed by solventogenic processes) for ethanol and butanol production could both improve solvent production and reduce the toxicity linked to acidogenic processes products [5,6].

The most important parameters influencing anaerobic solventogenic fermentations include pH, organic acids, nutrient limitation, temperature, oxygen and the source of inoculum [1,5,7]. Most of the studies performed on ethanol and butanol production through anaerobic solventogenic processes focussed on

using sugars as carbon source, and on using bacterial pure cultures, with the most studied bacterial genera being *Thermoanaerobacter* under thermophilic conditions [8–16], and *Clostridium* [5,7,17–22].

Using microbial mixed cultures rather than bacterial pure cultures for the production of alcohols from wastes through biological processes is of great interest. It increases the stability to the process, improves the resistance to both toxicity and microbial contaminations, and brings a higher substrate flexibility [23,24]. However, to date there is still a lack of fundamental knowledge on microbial mixed cultures used as inoculum, especially when H_2 is used as electron donor for the conversion of organic acids through solventogenic processes. Characterization of microbial communities capable of performing such processes is thus preponderant.

Enhancement of microbial communities through pretreatment of the inoculum is an effective way to induce changes in the communities that will improve process performance. This approach has already been successfully tested, but mainly for the optimization of the acidogenic step in H_2 production through anaerobic dark fermentation [25–35]. Pretreatments used in those studies consisted in modifications of the pH and temperature applied to the inoculum. Since microbial communities involved in acidogenic processes could use H_2 as electron donor to shift their metabolism to produce alcohols [1,4,36], the same inoculum pretreatments could be applied to improve solventogenic processes.

The present work evaluated the effects of four pretreatments of a microbial mixed population (acidic, thermal, acidic-thermal and thermal-acidic) on its capacity to convert VFAs into alcohols, using H_2 as electron donor and an equimolar mixture of acetate and butyrate as carbon sources. The composition and dynamics of the microbial mixed community were analysed.

4 Materials and Methods

4.1 Medium

The carbon source was an equimolar mixture of acetate and butyrate (17 mmol·L^{-1}, which correspond to 1,000 and 1,476 mg·L^{-1} of acetate and butyrate, respectively). The nutrient medium (micro and macro) composition was set accordingly to Angelidaki et al. [37] as described in Table 1. The initial pH was adjusted to 6.0.

Table 1 – Nutrients composition of the medium [37].

Nutrient	Concentration	Nutrient	Concentration	Nutrient	Concentration
NH_4Cl	1 g·L^{-1}	$MnCl_2{\cdot}4H_2O$	50 µg·L^{-1}	$(NH_4)_6Mo_7O_{24}{\cdot}4H_2O$	50 µg·L^{-1}
NaCl	100 mg·L^{-1}	$AlCl_3$	50 µg·L^{-1}	Pyridoxine Chloride	10 µg·L^{-1}
$MgCl_2{\cdot}6H_2O$	100 mg·L^{-1}	$CoCl_2{\cdot}6H_2O$	50 µg·L^{-1}	HCl Concentrated	1 µL·L^{-1}
$CaCl_2{\cdot}2H_2O$	50 mg·L^{-1}	$NiCl_2{\cdot}6H_2O$	92 µg·L^{-1}	$Na_2SeO_3{\cdot}5H_2O$	100 µg·L^{-1}
$K_2HPO_4{\cdot}3H_2O$	400 mg·L^{-1}	EDTA	500 µg·L^{-1}	Nicotinic acid	5 µg·L^{-1}
$FeCl_2{\cdot}4H_2O$	2 mg·L^{-1}	Biotin	2 µg·L^{-1}	Pantothenic acid	5 µg·L^{-1}
H_3BO_3	50 µg·L^{-1}	Riboflavin	5 µg·L^{-1}	B_{12} Vitamin	0.1 µg·L^{-1}
$ZnCl_2$	50 µg·L^{-1}	Thiamine	5 µg·L^{-1}	p-aminobenzoic acid	5 µg·L^{-1}
$CuCl_2{\cdot}2H_2O$	38 µg·L^{-1}	Folic acid	2 µg·L^{-1}	Thioctic acid	5 µg·L^{-1}

4.2 Inoculum

The sludge used as inoculum in all assays was a primary digestate of the Carleton Corner Farms (Marionville, ON, Canada) collected in May, 2013. The sludge was sieved 3 times using a 2 mm mesh sieve to eliminate all inert and heterogeneous lignocellulosic materials. The total volatile solids (TVS) content of the sieved sludge was of 41 ± 3 mg TVS·L^{-1}. The sludge was centrifuged (SorvalTM RC 6 Plus, Thermo Inc.) 40 min at 10k min^{-1} and at 5°C. Supernatant was discarded and the pellet was ressuspended in a phosphate buffer (500 mg·L^{-1} PO_4^{3-}), using a homogenizer and disperser

(Ultraturrax^{TM} T25, IKA Inc.) for 10 min at 15k·min^{-1}. The sludge was then sonicated to disaggregate possible granules and biofilms, using a sonicator (Vibra Cell^{TM} VC130, Sonics Inc.) with 30W of power. This step was repeated 4 times, on ice, with a time/volume dependence relation of 4 s·mL^{-1}, with 2 minutes of interval between sonications. These steps were carried out to ensure the homogeneity of the inoculum and to wash possible organic dissolved materials present in the sludge, which could be used as an alternative carbon source during the process. The pH was corrected to 6.0 using a 1.0 M solution of HCl under vigorous stirring. This processed sludge was considered as the control inoculum.

4.3 Pretreatments

Four different physicochemical pretreatments – acidic, thermal, acidic-thermal, and thermal-acidic – were performed on the control inoculum. Pretreated inocula were then compared to each other, using the control inoculum as reference. In addition to each pretreatment, all inocula were submitted, prior to inoculation, to a starvation process to reduce the length of the lag phase. This step consisted in incubating the inoculm for 72 hours at 30°C, under an agitation of 50 min^{-1}. The control inoculum was submitted to the same starvation process and presented a TVS content of 31 ± 0 mg TVS·L^{-1}.

The acidic pretreatment consisted in decreasing the pH down to 3.0, with a 12 M HCl solution under stirring, followed by an incubation of 24 hours at 30°C, under an agitation of 50 min^{-1}. pH was controlled every hour for the 5 first hours to assure its stability. After incubation, the pH was increased up to 6.0 with a 2 M NaOH solution under stirring, followed by an incubation of 24 hours at 30°C under an agitation of 50 min^{-1}. pH was controlled every hour for the 5 first hours to assure its stability. The acidic pretreated inoculum had a TVS of 29 ± 1 mg TVS·L^{-1}.

The thermal pretreatment consisted in heating the control inoculum at 90°C for 20 minutes, under stirring and using a water batch. The inoculum was then immediately transferred to an ice batch until it reached room temperature (23°C). The thermal pretreated inoculum had a TVS of 31 ± 0 mg TVS·L^{-1}.

The acidic-thermal and thermal-acidic pretreatments consisted in performing sequentially the two pretreatments as indicated by the name. The second pretreatment was performed immediately after the first one. The acidic-thermal pretreated inoculum had a TVS of 36 ± 3 mg TVS·L^{-1} and thermal-acidic pretreated inoculum had a TVS of 32 ± 0 mg TVS·L^{-1}.

4.4 Experimental Setup

Initial physicochemical parameters for each experiment (pretreatment and control) are shown in Table 2. Each experiment was carried out in quintuplicates, using 538 ± 3 mL sealed glass bottles, with an initial working volume of 110 mL. All the bottles were incubated upside down, to avoid any diffusion of H_2 through bottle's cap, at 30°C under an agitation of 150 min^{-1}. At the beginning of each experiment, the headspace of each bottle was totally replaced by pure H_2 (99.99%) at a pressure of 2.39 ± 0.08 atm (242.2 ± 7.9 MPa). Such headspace replacement was repeated after each sampling to ensure a constant pressure and composition all along the experiment.

Table 2 – Initial conditions (prior to inoculation) for each assay.

Assay	pH	Acetate mg·L^{-1}	Butyrate mg·L^{-1}	Inoculum mg TVS·L^{-1}	Total H_2 mmol	Dissolved H_2* mmol·L^{-1}
Control	5.89	1153	1727	11.3 ± 0.2 (5)	37.9 ± 1.6 (5)	1.69
Acidic	5.94	1139	1708	11.0 ± 0.2 (5)	39.2 ± 0.2 (5)	1.74
Thermal	6.07	1143	1712	12.8 ± 3.7 (5)	40.2 ± 0.1 (5)	1.78
Acidic-thermal	5.84	1233	1846	12.7 ± 0.2 (5)	40.8 ± 0.2 (5)	1.81
Thermal-acidic	5.85	1213	1816	11.3 ± 0.1 (5)	39.7 ± 1.3 (5)	1.77

Values in parenthesis are the number of replicates. * Dissolved H_2 was estimated through Henry's Law [38,39].

Initial analyses of the liquid phase confirmed the absence, at the beginning of the assay, of significant amounts of alcohols, mono or disaccharides, and fatty acids other than acetate and butyrate.

4.5 Physicochemical Analyses

pH monitoring was performed with a portable pHmeter (Accumet™ AP115, Fisher Scientific™), with a microprobe electrode (Accumet™ 55500-40, Cole Parmer™), using the method 4500-H^+ B, described by APHA [40]. TVS analyses were performed in quintuplicate, following method 2540-E, accordingly to APHA [40]. Pressure inside the bottles was measured using a digital manometer (DM8200, General Tools & Instruments™) with a range pressure of 0 - 6,804 atm (689.5 MPa). Dissolved CO_2 was measured through alkalinity determination by potentiometric titration [41,42].

Mono, disaccharides and organic fatty acids were analyzed using a Waters™ HPLC, which consisted in a pump (model 600) and an autosampler (model 717 Plus). The system was equipped with a refractive index detector (model 2414), for mono and disaccharides analyses. Organics acids were monitored from the same samples using the same equipment, through a linked photo diode array detector (model 2996). A Transgenomic™ ICSep IC-ION-300 (300 mm x 7.8 mm outer diameter) column was used for separation of all compounds, and was operated at 35°C. The mobile phase was 0.01 N H_2SO_4 at 0.4 $mL \cdot min^{-1}$ under an isocratic flow.

Alcohols (methanol, ethanol, acetone, 2-propanol, tert-butanol, n-propanol, sec-butanol, and n-butanol) were measured on an Agilent™ 6890 gas chromatograph (GC) equipped with a flame ionization detector, as described by Guiot *et al.* [43].

100 µL gas samples, obtained using a gas-tight syringe (model 1750, Hamilton™), were used for gas composition (H_2, CO_2, CH_4 and N_2) measurements with a GC (HP 6890, Hewlett Packard™) equipped with a thermal conductivity detector (TCD) and a 11 m x 3.2 mm 60/80 mesh packed column (Chromosorb™ 102, Supelco™). The column temperature was held at 50 ºC for the entire run (4 min). The carrier gas was argon. The injector and detector were maintained at 125°C and 150°C respectively.

4.6 16S rRNA gene Sequencing and microbial characterization

Bacterial 16S rRNA genes (V2 region) were amplified using the set of primers 16S-F343 IonA L01 (343-357; 5′ TACGGRAGGCAGCAG 3′) and 16S-R533 Ion P1 (516-533; 5′ ATTACCGCGGCTGCTGGC 3′) [44]. A sample-specific multiplex identifier was added to each forward primer and a Ion Torrent adapter to each primer. DNA extraction was conducted accordingly Griffiths *et al.* [45]. DNA was then purified following procedures described by Lévesque *et al.* [46] and Berthelet *et al.* [47]. Amplification reactions were performed in a final volume of 20 µL, which contained 1 µL of DNA, 0.5 µM of each primer, 7.5 µL of RNAse free H_2O and 10 µL of 2X HotStarTaq™ Plus Master Mix (HotStarTaq™ *Plus* Master Mix Kit, Qiagen, USA). PCR conditions were an initial denaturation of 5 min at 95°C followed by 25 cycles of 30 s at 95°C, 30 s at 55°C, and 45 s at 72°C, with a final elongation step of 10 min at 72°C. PCR products were purified and quantified using respectively a QIAquick™ gel extraction kit (Qiagen, USA) and a Quant-iT PicoGreen™ double-stranded DNA quantitation kit (Life Technologies Inc., USA), according to manufacturer's instructions. The pooled amplicons were then sequenced using the Ion Torrent™ (Life Technologies Inc., USA) sequencing platform with a 314 chip, according to manufacturer's instructions. Bacterial 16S rRNA gene sequences generated were and analyzed using the ribosomal database project (RDP) classifier [48], using a bootstrap confidence cutoff of 50%, as recommended by RDP classifier [49] for short sequences (less than 250 bp). Prior to analysis, sequences shorter than 75 bp and sequences with unidentified bases (N) were removed.

4.7 Kinetics

Equation fitting of results for both ethanol and butanol production, was performed by applying a modified Boltzmann sigmoidal model, as shown by Equation 1. The model was modified to incorporate the parameter as maximum rate of the process (mg L^{-1} h^{-1}).

Equation 1

Where is the function of concentration in respect of time (mg L^{-1}), is time (h), is the maximum concentration reached (mg L^{-1}), and is the value of time when (h).

The length of the lag and exponential phases were estimated assuming the exponential phase as a linear equation, with as its slope. Length of the lag phase (, h) was considered when, as its ending time (, h) was considered when. The length of exponential phase (, h) is the difference between these times (- , h). Equation 3 and 4, respectively, define and .

Equation 3

Equation 4

All fitting were performed using the software Microcal Origin Pro^{TM} 9.0, using a Levenberg-Marquardt algorithm for fitting and initializing the equations parameters.

4.8 Metabolisms' Gibb's free energy

Gibb's free energy values were calculated for all pathways depicted in Figure 1, with the exception of pathway 1, for both initial (ΔG^{I}_{r}) and final (ΔG^{F}_{r}) conditions, and were compared with the free energy for standard conditions (ΔG^{o}_{r}). ΔG^{o}_{r} values for each reaction were estimated as previously described [50,51], considering 1 mol of each product and reagent at STP. ΔG^{I}_{r} and ΔG^{F}_{r} values were calculated using the Nernst equation, at 30 °C, and took into account the metabolites concentrations presented in Table 4. Compounds which were not detected in the beginning of the experiments, such as butanol, propionate, propanol and ethanol, were assumed to be present at very low concentrations ($<10^{-3}$ mmol

L^{-1}). In all studied conditions, CO_2, which was not detected at the end of any experiment, was considered constant and very low ($<10^{-1}$ mmol L^{-1}) for the calculation of ΔG^F_r.

5 Results and Discussion

5.1 Metabolic Model and Molar Balances

For all experiments, gas composition of the headspace was monitored prior to its replacement and H_2 pressure was constantly kept at 2.15 ± 0.10 atm. H_2 was the only gas detected in the headspace in all cases, except for the control experiment, for which a methane production of 0.24 mmol (5.37 mL at standard temperature and pressure (STP)) was observed. Initial and final concentrations of the main metabolites (added or produced) and of dissolved H_2 and CO_2 are presented in Table 3. Dissolved H_2 was not measured but estimated through Henry's law [38,39], and its concentration was considered constant, due to its continuous replacement. Dissolved CO_2 was calculated from the alkalinity value measured at the beginning of each assay. CO_2, O_2 and N_2 were never detected. Acetone, lactate and methanol were only sporadically detected in the liquid phase, in traces concentrations (below 1 $mg \cdot L^{-1}$). Neither propionate nor alcohols were detected at the beginning of each experiment.

Table 3 – Mean concentrations of all metabolites detected and of dissolved H_2 and CO_2.

Metabolite[a]	Concentration (mg L^{-1})									
	Control		Acidic		Thermal		Acidic-thermal		Thermal-acidic	
	Initial	Final	Initial	Final	Initial	Final	Initial	Final	Initial	Final
Acetate	1225 ± 1	1575 ± 40	1222 ± 3	1492 ± 24	1206 ± 2	1722 ± 120	1235 ± 3	1645 ± 44	1224 ± 2	1447 ± 26
Butyrate	1831 ± 3	1773 ± 24	1828 ± 1	1935 ± 14	1791 ± 4	1796 ± 17	1840 ± 5	1664 ± 25	1831 ± 4	1738 ± 58
Propionate	-	42 ± 12	-	35 ± 4	-	107 ± 25	-	52.8 ± 9.2	-	40.1 ± 5.4
Ethanol	-	40 ± 6	-	14 ± 2	-	104 ± 7	-	94 ± 9	-	33 ± 6
Propanol	-	-	-	0.3 ± 0.2	-	-	-	1.8 ± 0.1	-	1.0 ± 0.3
Butanol	-	49 ± 8	-	11 ± 2	-	83 ± 3	-	154 ± 14	-	61 ± 25
Dissolved H_2	-	1.6 ± 0.1	-	1.7 ± 0.0	-	1.6 ± 0.1	-	1.7 ± 0.1	-	1.7 ± 0.1
Dissolved CO_2	-	3.07	-	2.40	-	3.30	-	1.56	-	2.19
Duration (d)	29.2		29.1		29.1		29.1		29.0	

[a]All values are expressed in mg·L^{-1} except for dissolved H_2 and CO_2 expressed in mmol·L^{-1}. Mean concentrations of acetate, butyrate, propionate and butanol for 5 replicates, and of dissolved H_2 for 50 samples.

Monitoring acetate and butyrate along the process demonstrated a production of acetate in all cases, and only minor variations of butyrate concentrations (slight decrease for the control and the acidic-thermal and thermal-acidic pretreatments, low production for the acidic and the thermal pretreatments). Such results suggested an alternative organic matter input in the system. This is consistent with the decrease of the concentration of total volatile solids (TVS) that was observed for all conditions tested , as a direct effect of the different pretreatments on the biomass, which might have resulted in partial microbial cell death. Such non-living cells constituted non-soluble organic matter which was probably hydrolysed and then consumed as a supplementary carbon source. Based on well-known anaerobic acidogenic and solventogenic metabolisms [1,36], and considering the inoculum as the only possible alternative source of organic matter, an alternative metabolic model including such contribution and considering the main metabolites (added and produced) presented in Table 3, was developed (Figure 1).

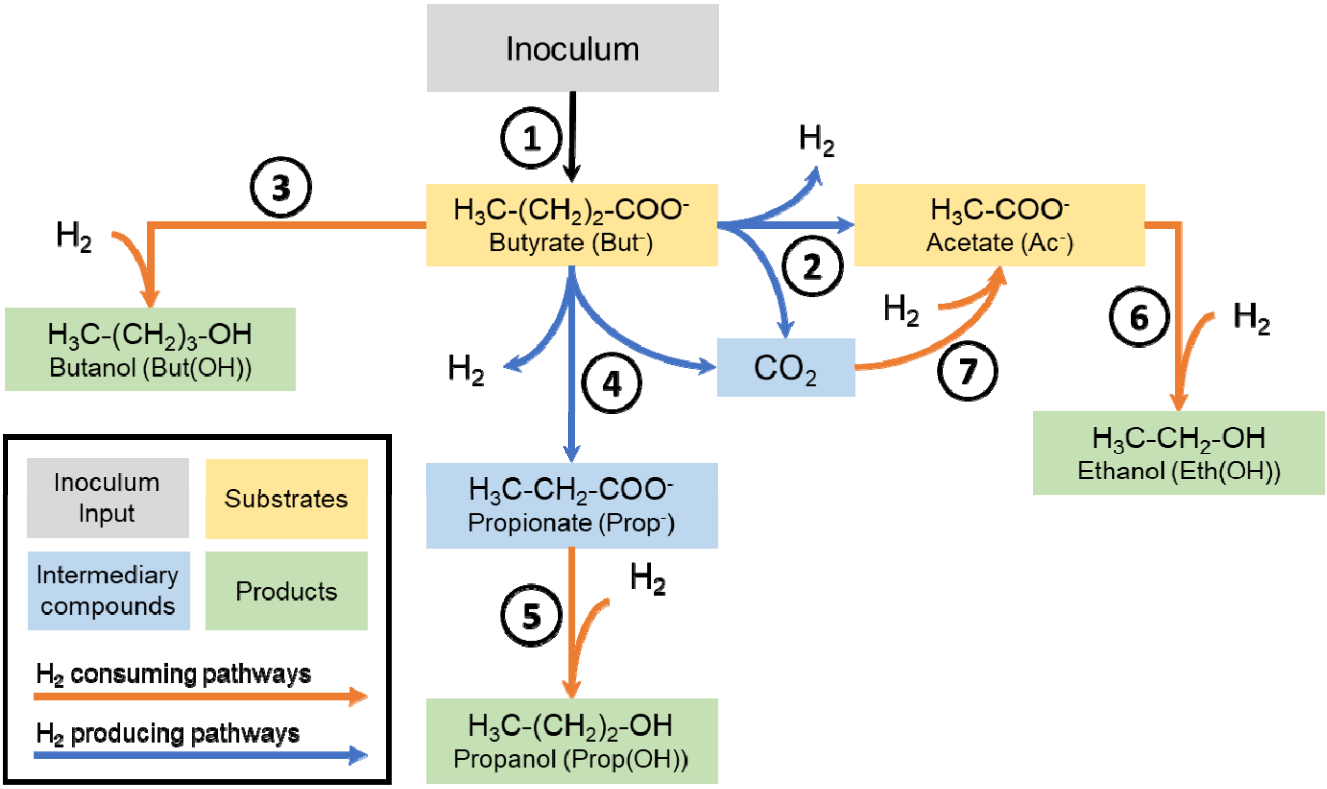

Metabolic Pathways

1	Organic matter in the inoculum to butyrate	
2	Acetogenesis from butyrate	$But^- + 4H_2O \rightarrow Ac^- + 2CO_2 + 6H_2$
3	Solventogenesis from butyrate to butanol	$But^- + H^+ + 2H_2 \rightarrow But(OH) + H_2O$
4	Acidogenesis from butyrate to propionate	$But^- + 2H_2O \rightarrow Prop^- + CO_2 + 3H_2$
5	Solventogenesis from propionate to propanol	$Prop^- + H^+ + 2H_2 \rightarrow Prop(OH) + H_2O$
6	Solventogenesis from acetate to ethanol	$Ac^- + H^+ + 2H_2 \rightarrow Eth(OH) + H_2O$
7	Homoacetogenesis	$2CO_2 + 4H_2 \rightarrow Ac^- + H^+ + 2H_2O$

Figure 1 – Alternative metabolic model proposed for the solventogenic process using butyrate and acetate as substrates. Pathways in orange are exergonic; pathways in blue are endergonic (at 30 °C, pH of 6.0, with a constant CO_2 concentration of 10^{-3} mmol L^{-1}, in initial conditions as depicted in Table 3).

This metabolic model was used to perform a molar balance of all carbon inputs and outputs during the process (Table 4). All balances were performed on a 1 L basis and derived from initial and final

experimental values obtained in all conditions (Table 3), except for the organic matter from the inoculum (pathway 1) which was expressed in butyrate equivalent.

Table 4 – Molar balance of all metabolites detected in all metabolic pathways of each experiment.

Metabolite	Pathway[a]	Molar Balance (mmol)[b]				
		Control	Acidic	Thermal	Acidic-thermal	Thermal-acidic
Butyrate	Initial*	21.0	21.0	20.6	21.1	21.0
	Final*	20.4	22.2	20.6	19.1	20.0
	1	***+ 4.69***	***+ 4.76***	***+ 8.57***	***+ 5.51***	***+ 3.05***
	2	- 4.06	- 2.93	- 5.99	- 4.70	- 2.67
	3	- 0.66	- 0.15	- 1.12	- 2.08	- 0.82
	4	- 0.57	- 0.48	- 1.46	- 0.75	- 0.57
Butanol	3*	+ 0.66	+ 0.15	+ 1.12	+ 2.08	+ 0.82
Propionate	4	+ 0.57	+ 0.48	+ 1.46	+ 0.75	+ 0.57
	5	-	-	-	- 0.03	- 0.02
Propanol	5*	-	-	-	+ 0.03	+ 0.02
Acetate	Initial*	20.7	20.7	20.4	20.9	20.7
	Final*	26.7	25.3	29.2	27.9	24.5
	2	+ 4.06	+ 2.93	+ 5.99	+ 4.70	+ 2.67
	6	- 0.87	- 0.30	- 2.26	- 2.04	- 0.72
	7	+ 2.81	+ 1.97	+ 5.07	+ 4.30	+ 1.85
Ethanol	6*	+ 0.87	+ 0.30	+ 2.26	+ 2.04	+ 0.72
Dissolved CO_2	2	+ 8.12	+ 5.86	+ 12.0	+ 9.41	+ 5.33
	4	+ 0.57	+ 0.48	+ 1.46	+ 0.75	+ 0.57
	7	- 5.62	- 3.94	- 10.14	- 8.59	- 3.71

*Values obtained experimentally (derived from initial and final concentrations as indicated in Table 3).
[a]Metabolic pathways described in Figure 1.
[b]Balance on a 1 L basis; "+" indicates a production; "-" indicates a consumption.

According to our model, CO_2 was produced by the conversion of butyrate into acetate (pathway 2) and by acidogenesis of propionate from butyrate (pathway 4). This CO_2 was then entirely consumed to form acetate through a homoacetogenic pathway (pathway 7). This hypothesis was supported by the absence of CO_2 detection in any experiment and by the increase of acetate concentration in all

experiments. This may be linked to microbial communities more adapted to the conversion of both butyrate and CO_2 into acetate (pathways 2 and 7) rather than to the conversion of acetate into ethanol (pathway 6). Our alternative metabolic model also indicates that butyrate was mainly consumed to produce acetate (pathway 2) in all studied conditions, and that organic matter from the inoculum (pathway 1) represented an important external input, since butyrate concentrations decreased only slightly or increased. Ethanol and butanol were produced (pathways 3 and 6) in all experiments, with the highest concentration (at least 100 mg L^{-1}) being observed for the thermal and acidic-thermal pretreatments. Although acidogenesis of propionate from butyrate (pathway 4) was active in all conditions, with the highest yield obtained with the thermal pretreatment, propanol, from the conversion of propionate (pathway 5), was only obtained with the acidic, acidic-thermal and thermal-acidic pretreatments.

The successful closure of molar balances, with a stoichiometrically balanced sum of all inputs and outputs when considering the contribution of the inoculum, indicates that our alternative metabolic model accurately represents the solventogenic processes occurring in all studied conditions. To reinforce this hypothesis, Gibb's free energy values were calculated for each pathway, for both initial and final conditions (Figure 2). Those values, providing an overview of the thermodynamic feasibility of each pathway involved in the solventogenic process, tend to validate our model depicted in Figure 1.

Metabolic Pathway	Metabolism Free Energy (kJ mol^{-1})									
	ΔG^{o}_{r}	Control		Acidic		Thermal		Acidic-thermal		Thermal-acidic	
		ΔG^{I}_{r}	ΔG^{F}_{r}	ΔG^{I}_{r}	ΔG^{F}_{r}	ΔG^{I}_{r}	ΔG^{F}_{r}	ΔG^{I}_{r}	ΔG^{F}_{r}	ΔG^{I}_{r}	ΔG^{F}_{r}
2	109	-165	224	-165	220	-165	226	-165	227	-165	222
3	-20,6	-291	-129	-291	-168	-290	-116	-291	-99	-291	-123
4	55,7	-329	214	-329	211	-328	194	-329	192	-329	204
5	-24,4	-47	-205	-47	-201	-47	-228	-47	-126	-47	-135
6	-20,5	-290	-5	-290	25	-290	-17	-291	-51	-290	-19
7	-40	332	-60	332	-49	332	-62	333	-25	332	-46

Figure 2 – Gibbs' free energy for initial (ΔG^{I}_{r}), final (ΔG^{F}_{r}) and standard (ΔG^{o}_{r}) conditions for each pathway (as defined in Figure 1) in each experiment. Green values (< 0) are exergonic; yellow values (nul) are in equilibrium; red values (> 0) are endergonic.

Monitoring energetic profiles could help to anticipate changes within metabolisms. As shown in Figure 2, the estimated ΔG^{o}_{r} values indicate that acetogenesis of acetate from butyrate and acidogenesis of propionate from butyrate (pathways 2 and 4, respectively) are theoretically thermodynamically unfeasible reactions. In all conditions tested in this study, those reactions evolved to become thermodynamically feasible. Acetogenesis from butyrate (pathway 2) was likely inhibited in the beginning of each experiment due to the concentration of dissolved H_2 and CO_2. H_2 and CO_2 were progressively consumed through homoacetogenesis (pathway 7), which progressively rendered pathway 2 thermodynamically feasible. At low concentrations of dissolved CO_2, the homoacetogenesis pathway became thermodynamically unfeasible. Such metabolisms evolution could explain the production acetate observed in all studied conditions, all along the process. Metabolic pathways 3 (solventogenesis of butanol) and 6 (solventogenesis of ethanol) were thermodynamically feasible in all studied conditions all along the process, explaining the observed production of such alcohols.

Metabolic pathways 4 (acidogenesis of propionate) and 5 (solventogenesis of propanol) were thermodynamically feasible in all studied conditions too, however an energetic shift from production of propionate towards production of propanol was observed during the process.

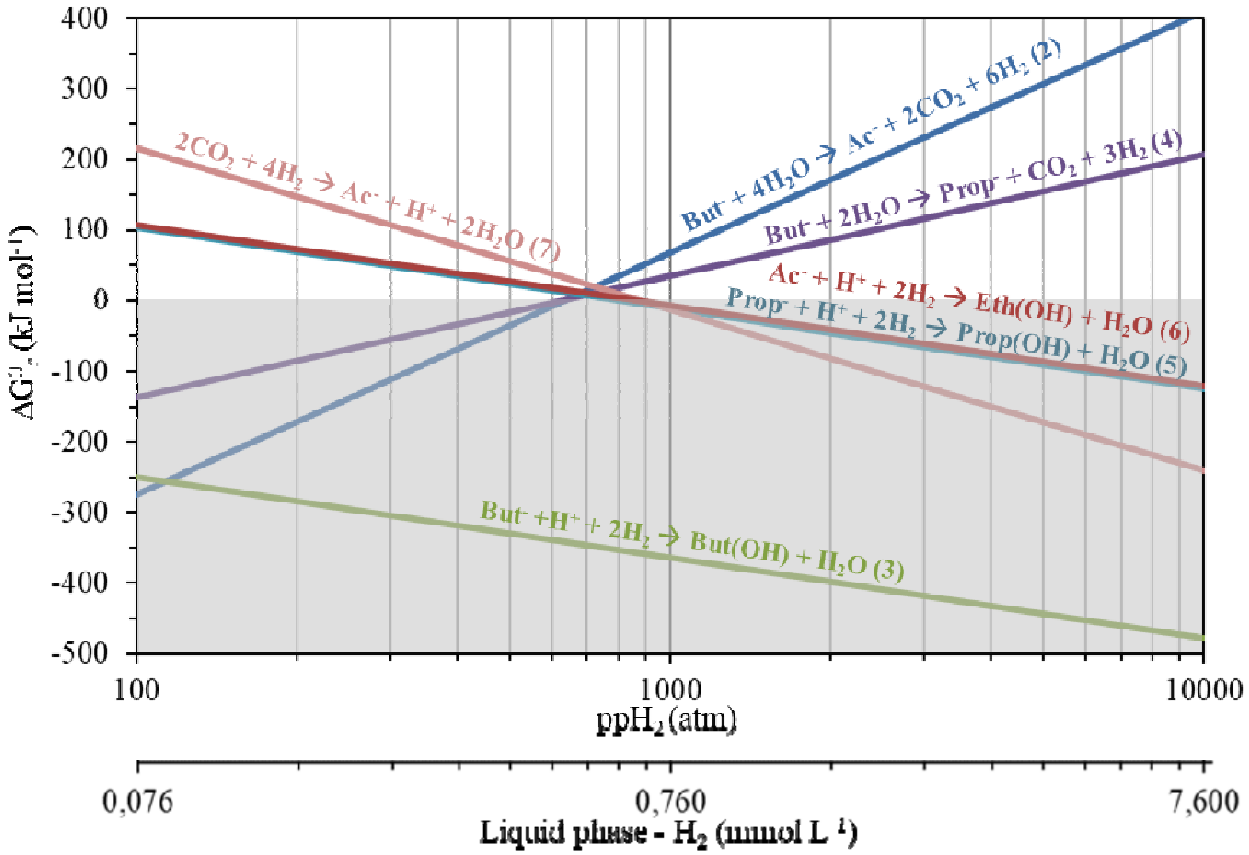

Figure 3 – Evolution of the standard Gibbs' free energy (ΔG^{o}_{r}) in function of the partial pressure of H_2. Evolution for each metabolic pathway (as defined in Figure 1), at 30 °C, and with a standard concentration of 1.0 mol L^{-1} for each reagent other than H_2. Shadowed area indicates thermodynamically feasible reactions.

As described previously, H_2 has a particularly important role as a co-substrate in the anaerobic process energetics [52,53]. As shown in Figure 3, solventogenesis of butanol from butyrate (pathway 3) is less sensitive to low pp_{H_2} than solventogenesis of ethanol and propanol, respectively from acetate (pathway 6) and propionate (pathway 5). By extrapolation, equilibrium ($\Delta G^{o}_{r} = 0$) in pathway 3 would be achieved at a pp_{H_2} of $4 \cdot 10^{-4}$ atm (43.7 Pa), implying that solventogenesis of butanol could theoretically

be carried out at very low pp_{H_2}. It is also possible to infer from Figure 3 that at pp_{H_2} higher than 0.62 atm (62.5 MPa), acidogenesis of propionate (pathway 4) and acetogenesis of acetate (pathway 2) from butyrate will stop, shutting down the production of acetate, propionate and H_2. In addition to low CO_2 concentrations, high pp_{H_2} thus represents an important factor that render such process thermodynamically feasible and favors solventogenesis from VFAs.

5.2 Alcohols and VFAs metabolisms

As shown in Figure 4, the highest concentrations of alcohols were obtained for both thermal and acidic-thermal pretreatments, with the best rate observed for the acidic-thermal pretreatment, especially for butanol production. On the opposite, the lowest alcohol production was observed for the acidic pretreatment. Evolution of acetate and butyrate concentrations confirmed the contribution of the inoculum as an important source of organic matter as substrate for alcohol production, since in all conditions tested, acetate concentration increased and butyrate concentration increased or only slightly decreased. These results reinforced the hypothesis described in Figure 1 and Table 4, of an acetate production through acetogenesis of butyrate (pathway 2) and homoacetogenesis (pathway 7), and preferentially through pathway 2 due to low concentrations of CO_2 in the beginning of all assays.

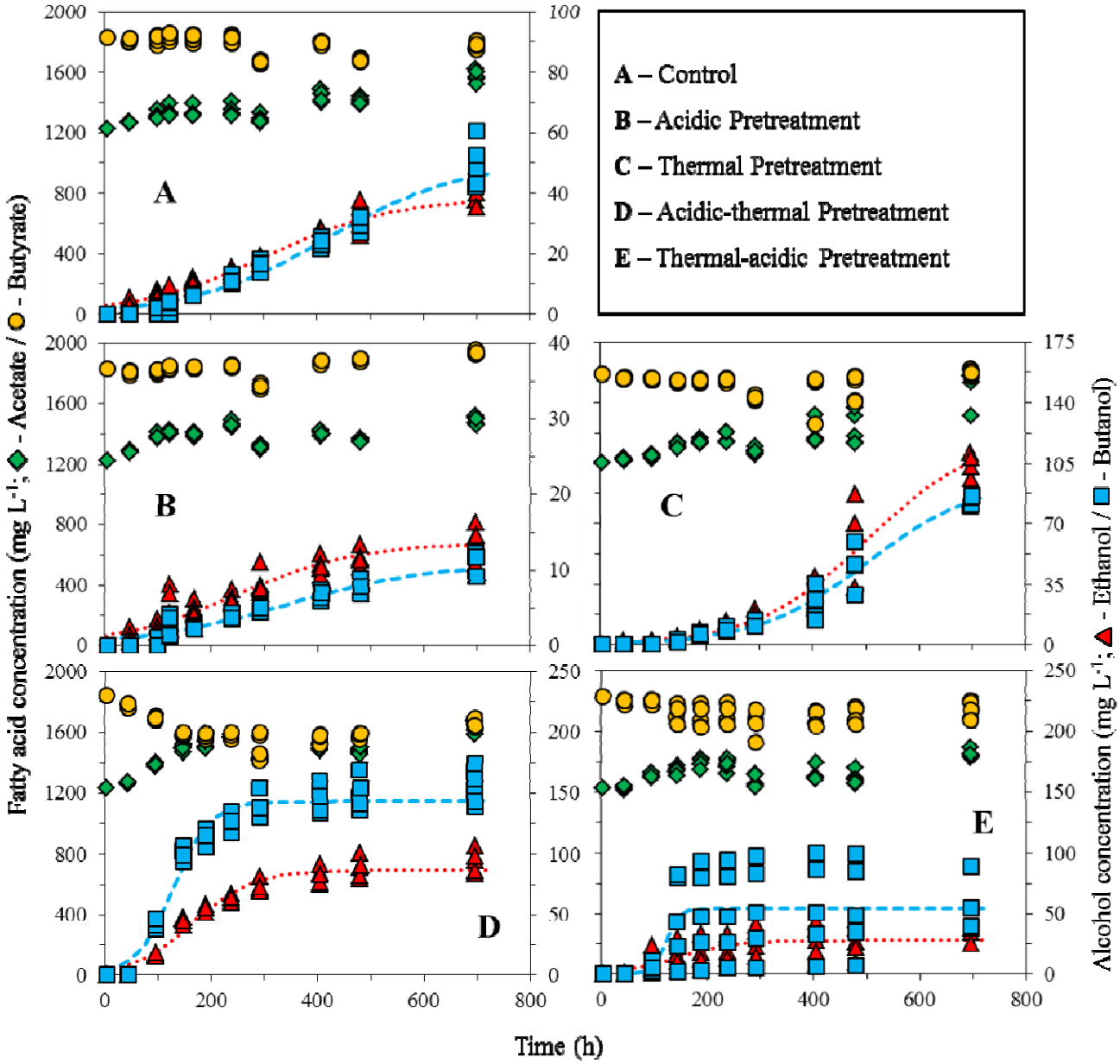

Figure 4 – Kinetics of VFAs (acetate and butyrate) and alcohols (ethanol and butanol) productions for each studied conditions. Red dotted- and blue dashed-lines represent the modified Boltzmann model fittings for ethanol and butanol concentrations, respectively.

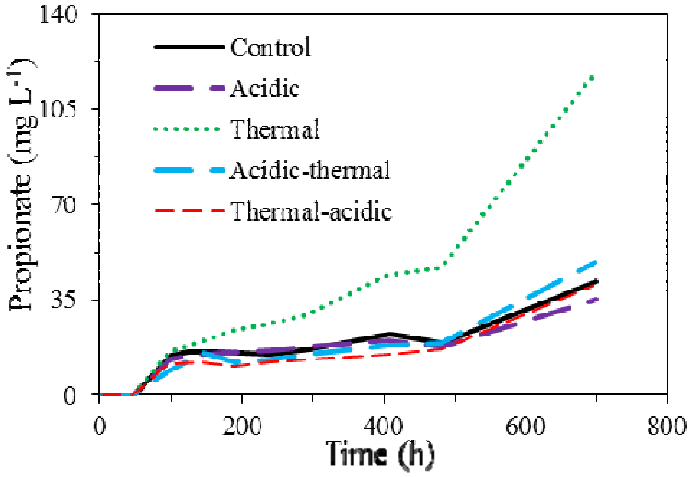

Figure 5 – Kinetics of propionate production for each studied conditions.

As shown in Figure 5, propionate was produced in all conditions tested. No significant difference was observed in the concentrations produced (42.4 ± 10.0 mg L^{-1}), with the exception of the thermal pretreatment assay, for which the level of production was 2.5 times higher than in all other conditions. As presented in Table 3, propionate was then consumed and converted into propanol (pathway 5 from Figure 1) for the acidic, acidic-thermal and thermal-acidic pretreatments. Despite the favourable thermodynamics of this reaction (Figure 2), propanol was only produced in trace amounts. Oxidation of propionate into acetate was considered unlikely since such reaction is energetically unfeasible in standard conditions (ΔG^{o}_{r} = 53.3 kJ mol^{-1}), and that, as previously described [39], at high H_2 concentrations, ΔG_r values are increased.

Table 5 presents the parameters of the modified Boltzmann model fitting the experimental data from Figure 4. Those parameters are related to the kinetics of alcohols production and allow the comparison of process efficiencies between all pretreatments in function of the time. A high correspondence was obtained between replicates for all conditions tested, with the exception of the thermal-acidic pretreatment. In that particular condition, the correlation coefficient was very low, only reaching 0.5 for ethanol and 0.4 for butanol, indicating that the process was unpredictable and could not be reproduced.

Due to its instability and unpredictability, the thermal-acidic pretreatment was thus no longer taken into consideration for analyses.

Table 5 – Parameters of the modified Boltzmann model fitting for ethanol and butanol production.

	Parameters	Pretreatment of the inoculum				
		Control	Acidic	Thermal	Acidic-thermal	Thermal-acidic
Ethanol	(mg L^{-1})	38.5 ± 1.5	13.6 ± 0.69	122 ± 10	87.3 ± 1.9	27.6 ± 2.8
	(h)	305 ± 14	249 ± 19	503 ± 26	166 ± 6	146 ± 25
	(mg L^{-1} h^{-1})	0.08 ± 0.00	0.03 ± 0.00	0.29 ± 0.02	0.39 ± 0.03	0.13 ± 0.05
	R^2	0.96	0.89	0.94	0.95	0.50
	(h)	64	22	293	54	38
	(h)	482	454	420	224	216
Butanol	(mg L^{-1})	50.7 ± 2.3	10.9 ± 0.52	96.7 ± 6.8	143 ± 2	53.8 ± 5.4
	(h)	422 ± 16	341 ± 18	506 ± 23	128 ± 4	122 ± 20
	(mg L^{-1} h^{-1})	0.10 ± 0.00	0.02 ± 0.00	0.23 ± 0.02	1.02 ± 0.09	1.11 ± 0.96
	R^2	0.97	0.94	0.96	0.96	0.40
	(h)	169	69	296	58	98
	(h)	507	545	420	140	48

, maximum concentration; , time when maximum production rate is achieved; , maximum production rate; R^2, correlation coefficient; and , initial and ending time of exponential growth phase.

As shown in Figure 4 and Table 3, the levels of alcohol production as well as the maximum rates of production () were improved for both thermal and acidic-thermal pretreatments. Despite the highest production of ethanol was observed for the thermal pretreatment, the best results were obtained for the acidic-thermal pretreatment, which allowed the best butanol production and an increase of 4.5 times of the ethanol maximum production rate and of 10.2 times of the butanol maximum production rate. In opposition, a strong decrease of alcohol production was observed for the acidic pretreatment. Such results clearly indicate that an acidic-thermal pretreatment of the inoculum is a promising approach for designing more efficient and smaller sized bioreactors.

Length of the lag phase () and duration of the bacterial exponential growth phase () were evaluated for each pretreatment and compared to the control by considering alcohol production curves as growth-associated curves (Table 3). The length of the lag phase is directly related to the time required for a bioreactor to initiate its process (start-up) and achieve higher rates of alcohol production. The shortest lag phases, for both ethanol and butanol production, were observed for the acidic and acidic-thermal pretreatments. In both pretreatments, the lag phase was shorter than the control's one. In opposition, the longest lag phase, which was considerably greater than the control's one for both ethanol and butanol production, was observed for the thermal pretreatment. Such results clearly indicate that the thermal pretreatment had the highest impact on the inoculum, while acidic and acidic-thermal pretreatments selected microbial communities which were the best adapted to solventogenic processes. Variations in the duration of the bacterial exponential growth phases () were also observed (Table 5). A shorter exponential growth phase is representative of a faster process. However, this parameter has to be evaluated concomitantly with the maximum rates of production (). For example, a short occurring at low indicates a process occurring with low efficiency. Among all the conditions tested, low values and high values were obtained for the acidic-thermal pretreatment, for both ethanol and butanol production. Taken all together, results obtained for all conditions tested indicate that the acidic-thermal pretreatment consisted in the best approach to generate a rapid and efficient process. ~~In the case of ethanol production, the higher value of found in acidic-thermal pretreatment when compared with thermal pretreatment condition (26.6% higher) was not enough to compensate the short , thus the thermal pretreatment was able to produce ethanol in a concentration 9.6% greater than in acidic-thermal pretreatment~~.

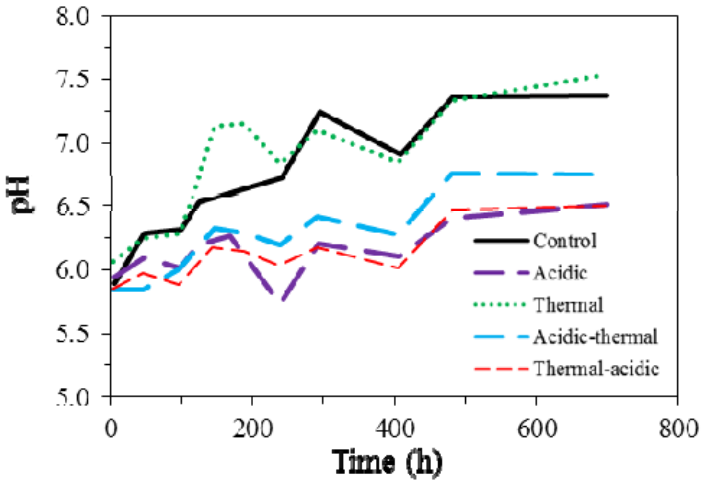

Figure 6 – Evolution of pH along the process for each studied conditions.

pH, which was initially set at a mean value of 5.92 ± 0.09, increased regularly all along the process for all conditions evaluated (Figure 6). This expected augmentation likely reflect the consumption of H_2, an electron donor, to form alcohols. Such pH increase occurred to a lesser extent for the acidic and acidic-thermal pretreatments. This difference might be explained by a more drastic initial pH drop resulting from the acidic fraction of the pretreatment, which lowered the buffer capacity of the inoculum. Such hypothesis was reinforced by the concentrations of dissolved CO_2, which were higher for both control and thermal pretreatment, as compared to acidic and acidic-thermal pretreatments (Table 3). Dissolved CO_2 concentration being directly related to the alkalinity, the lower concentrations observed in the acidic and acidic-thermal pretreatments reflect a reduced buffer capacity of the pretreated inocula.

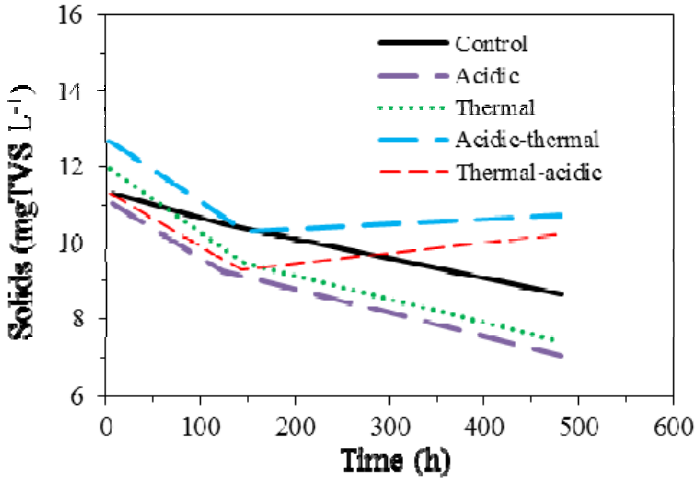

Figure 7 – Evolution of the total volatile solids (TVS) along the process for each studied conditions.

Finally, a decrease of the concentration of total volatile solids (TVS) was also observed for all conditions tested (Figure 7). This decrease is likely a direct effect of the different pretreatments on the biomass, which might have resulted in partial microbial cell death. Such non-living cells constituted non-soluble organic matter which was probably hydrolysed and then consumed as carbon source, contributing to the organic matter input as proposed in pathway 1 of Figure 1. The TVS concentration stopped decreasing and started to slightly increase after 150 hours in the acidic-thermal pretreatment. Such evolution is probably linked to the higher values of observed for this pretreatment (Table 5), which reflect an increase of the biomass growth's rate, and consequently TVS concentration.

5.3 Bacterial communities

Based on the results presented above, focusing particularly on alcohol production, both thermal and acidic-thermal pretreatments experiments were submitted to microbial community analyses. Bacterial populations were thus characterized and monitored all along those two processes. Thirteen phyla were detected, namely *Firmicutes*, *Proteobacteria*, *Bacteroidetes*, *Actinobacteria*, *Synergistetes*, *Cyanobacteria*, *Tenericutes*, *Spirochaetes*, *Deinococcus-Thermus*, *Fibrobacteres*, *Verrucomicrobia*,

Chloroflexi and *Nitrospirae*. Among those, three (*Firmicutes*, *Proteobacteria* and *Bacteroidetes*) represented up to 94.6% of the total OTUs detected in each sample for both pretreatments (Figure 8). *Firmicutes* was the most abundant phylum detected in the initial non treated inoculum (corresponding to 66.6% of the detected OTUs). Both pretreatments generated a shift in the bacterial population by stimulating the development of *Proteobacteria* and strongly reducing the number of *Firmicutes*. Bacterial populations evolved differently along the process for the two pretreatments. In the thermal pretreatment experiment (Figure 8A), a strong decrease of *Proteobacteria* was observed concomitantly with a strong increase of both *Bacteroidetes* and *Firmicutes*, the latest becoming the dominant phylum at the end of the process. This shift started after 200 hours of experiment, which correspond to the early beginning of the bacterial exponential growth phase (Figure 4C and Table 5). In opposition, in the acidic-thermal pretreatment experiment (Figure 8B), a relative stability was observed for the bacterial population, with *Proteobacteria* remaining the main phylum all along the process (72.0 ± 4.99% of the detected OTUs) and *Firmicutes* constantly being the second phylum of importance (24.0 ± 5.10% of the detected OTUs). *Bacteroidetes* increased regularly during the process, before starting to decrease after 500h of experiment, to reach at the end of the process their initial level.

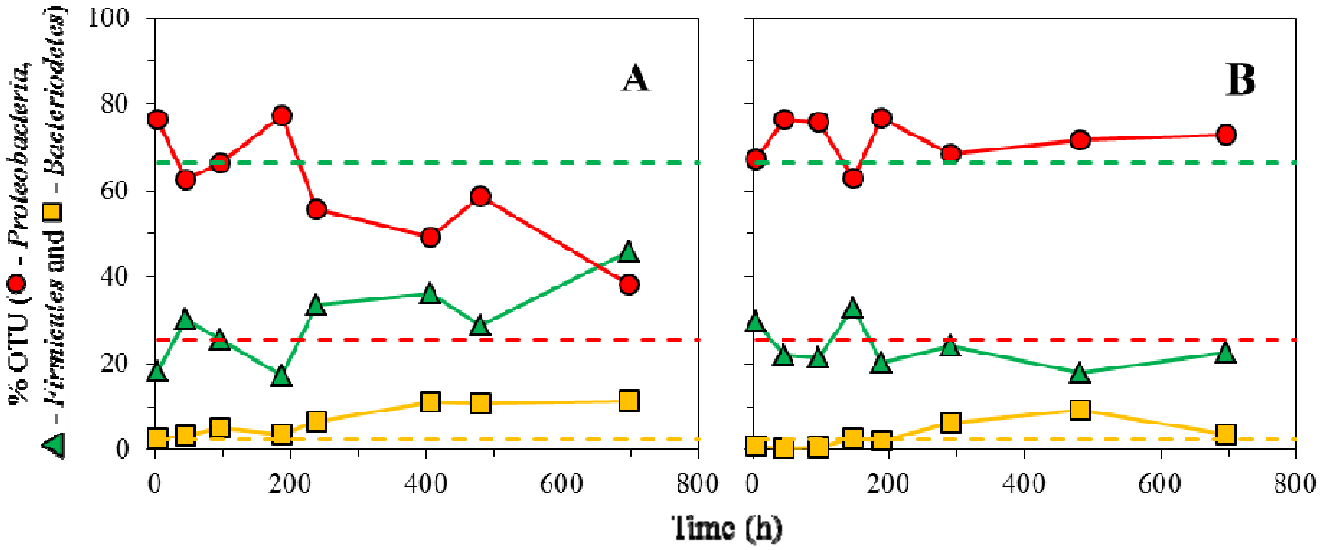

Figure 8 – Evolution of the three most representative bacterial phyla for the thermal (A) and acidic-thermal (B) pretreatments. Dashed lines represent OTUs associated to those same phyla in the control experiment (inoculum without pretreatment).

Deeper phylogenetic analyses were performed down to the genus level, in order to infer about potential metabolic pathway(s) that could be associated with the enhancement of alcohol production observed for both thermal and acidic-thermal pretreatments (Figure 9). Important differences were noticed between bacterial population from the initial inoculum (before any pretreatment) and those from the two pretreatments experiments.

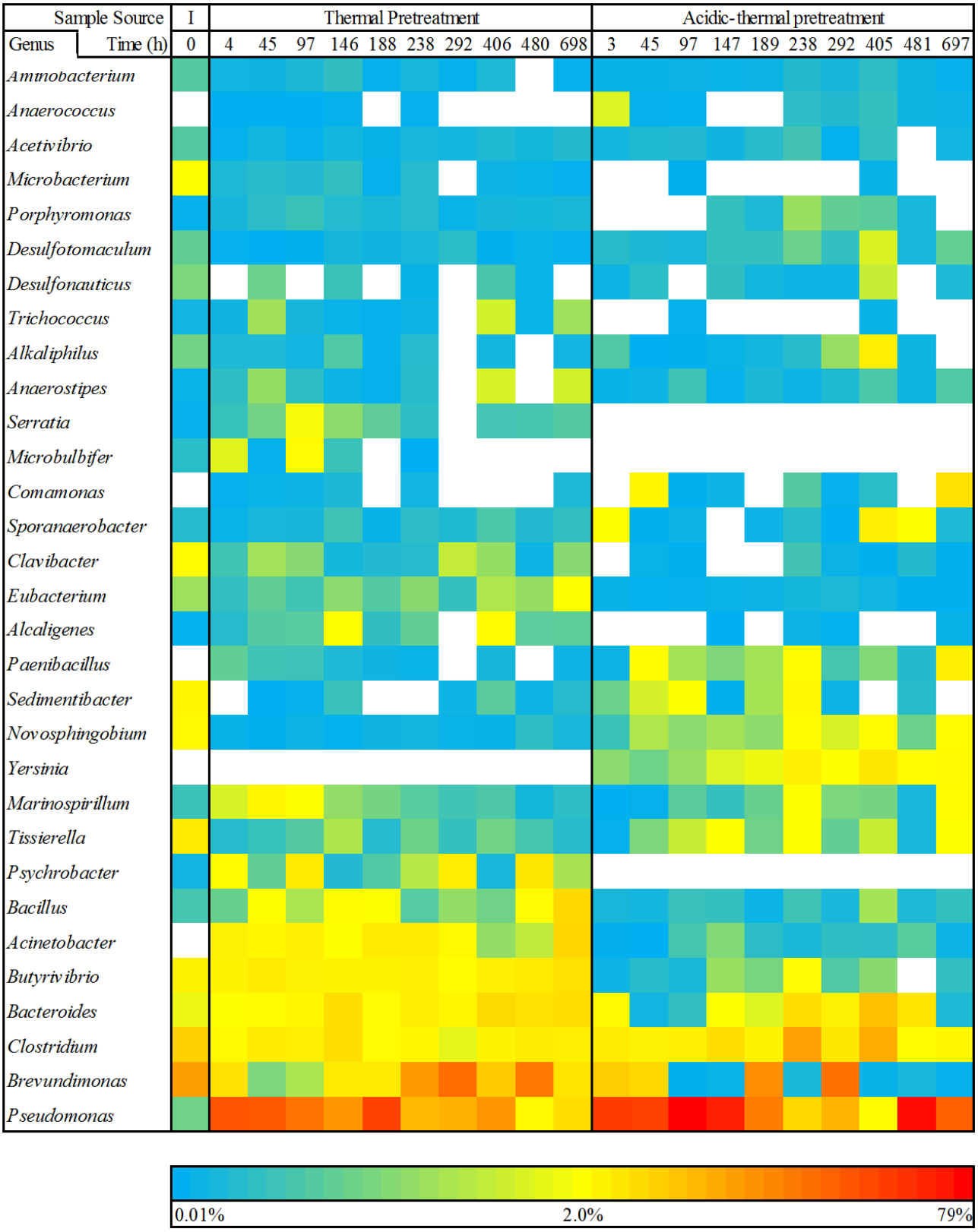

Figure 9 – Evolution of the bacterial population at the genus taxonomic level for thermal and acidic-thermal pretreatments, and comparison with the initial bacterial population (I) for the 31 most detected genera.

A total of 317 genera were detected in all samples tested, but only 31 of them, representing up to 85% of the bacterial population, were considered for further analysis (Figure 9). One of the most noticeable changes consisted in a strong increase of *Pseudomonas* in both pretreatment experiments, as compared to the initial population. Such increase was observed as soon as the first hours of experiments. *Pseudomonas* then remained a dominant genus of the bacterial population, despite a slight decrease observed for the thermal pretreatment in the second half of the process. Several *Pseudomonas* species have been genetically well-characterized, and have been shown to possess the genetic components for both ethanol (from pyruvate) and butanol (from glycerol and pyruvate) production [54]. Such prevalence of *Pseudomonas*, is thus likely linked with the higher levels of alcohol production observed in both thermal and acidic-thermal pretreatments. Some *Pseudomonas* species also possess genes responsible for the degradation of ethanol into acetyl-CoA [54]. This might explain the better butanol production, as compared to ethanol, observed for the acidic-thermal pretreatment. Among the other noticeable results, two bacterial genera, namely *Acinetobacter* and *Paenibacilus*, which were not detected in the initial population, appeared to be positively affected by both pretreatments. However, the growth of *Acinetobacter* was more stimulated for the thermal pretreatment, while the acidic-thermal pretreatment preferentially stimulated the growth of *Paenibacilus*.

In addition to those changes, several other bacterial genera evolved differently depending on the pretreatment applied (Figure 9). The thermal pretreatment appeared to better stimulate the growth of *Brevundimonas*, *Bacteroides*, *Butyrivibrio*, *Bacillus*, *Alcaligenes*, *Eubacterium*, *Clavibacter*, *Psychrobacter*, *Serratia* and *Microbulbifer*. The latter three being even exclusively detected in this pretreatment. On the opposite, the acidic-thermal pretreatment appeared to better stimulate the growth of *Tissierella*, *Novosphingobium*, *Sedimentibacter* and *Yersinia*. The latter one being exclusively detected in this pretreatment.

The genus *Brevudimonas* started to increase in the thermal pretreatment after 200h of process, coinciding with the very beginning of the exponential growth phase (Figure 4 and Table 5). Members belonging to this genus have already been shown to possess metabolic pathways related to acidogenesis of alcohols [55]. High H_2 partial pressures applied during the process might have rendered solventogenesis thermodynamically favorable through the reverse same metabolic pathway (Figure 3). The genus *Yersinia* started to increase in the acidic-thermal pretreatment after approximately 100 hours of process, coinciding with the early exponential growth phase (Figure 4 and Table 5). Members belonging to this genus have already been shown to possess metabolic pathways for the conversion of pyruvate into butanol and ethanol [54]. Finally, it noticeable that the genus *Clostridium*, which is composed by a high number of known alcohol producers through the conversion of glycerol and/or pyruvate into ethanol and/or butanol [18,56–58], was detected for both pretreatments all along the process, without any significant variations. This genus has thus likely an important role in the production of both ethanol and butanol in both thermal and acidic-thermal pretreatments.

Other results of interest were observed at higher taxonomic levels, notably highlighting a strong negative effect of both pretreatments on members of the family *Peptostreptococcaceae* and of the class *Epsilonproteobacteria*. The family *Peptostreptococcaceae*, which represented almost half (45% of total bacterial OTUs) of the bacterial community from the initial inoculum (before any pretreatment), strongly decreased down to 5.4 ± 2.2% in thermal and 9.2 ± 3.1% in acidic-thermal pretreatments. The class *Epsilonproteobacteria*, which represented up to 6% of total bacterial OTUs of the initial inoculum, significantly decreased down to less than 0.3% of total bacterial OTUs in both thermal and acidic-thermal pretreatments. Such results indicate that neither members of the family *Peptostreptococcaceae* nor members of the class *Epsilonproteobacteria* play a major role in the processes studied here.

6 Conclusions

Characterization of the initial microbial population showed the presence of bacteria possessing metabolic pathways for alcohols production. Both thermal and acidic-thermal pretreatments were able to select the best adapted bacterial communities to produce both ethanol and butanol. The significant decrease of members belonging to family *Peptostreptococaceae* coupled to the strong increase of *Pseudomonas* appeared to be related with the best performance in term of ethanol and butanol production. The acidic-thermal pretreatment generated the best results, reaching a concentration of 87 mg L^{-1} of ethanol and of 143 mg L^{-1} of butanol, after 240 hours of process. The thermal pretreatment achieved the highest production of ethanol (122 mg L^{-1}) but with a much slower rate (after 710 hours of process). The two other pretreatments studied showed either instability and inconsistency for the thermal-acidic pretreatment, or very low alcohol production for the acidic pretreatment. Among the VFAs added to the medium, only butyrate was used as substrate, acetate being produced along the process. Mass balance study highlighted another substrate input, which was probably originating from the inoculum. Thermodynamic data indicated that homoacetogenesis was an important pathway for the production of acetate from dissolved CO_2 and H_2. Finally, H_2 partial pressure was a preponderant factor for solventogenesis to occur, enabling alcohol production and inhibiting its consumption.

7 List of Abbreviations Used

STP	Standard temperature and pressure (0° C and 1 atm);
ppH_2	Partial H_2 pressure (átm);
R^2	Levenberg-Marquardt algorithm correlation coefficient;
TVS	Total volatile solids (mg L^{-1});
OTU	Operational taxonomic unit;
HPLC	High performance liquid chromatography;
PCR	Polimerase chain reaction;
RDP	Ribossomal data project;
VFA	Volatile fatty acid;
HBut	Butyrate;
HProp	Propionate;
HAc	Acetate;
But(OH)	Butanol;
Prop(OH)	Propanol;
Eth(OH)	Ethanol;
	Concentration in respect of time (mg L^{-1});
	Time (h);
	Initial time for exponential growth phase (h);
	Ending time for exponential growth phase (h);
	Time in which maximum production rate () is achieved (h);
	Maximum production rate (mg L^{-1} h^{-1});
	Maximum concentration (mg L^{-1});
ΔG_r	Variation of Gibbs' free energy at a given condition (kJ mol^{-1});
ΔG°_r	Variation of Gibbs' free energy at standard condition (kJ mol^{-1});
ΔG^{F}_r	Variation of Gibbs' free energy at final experiment condition (kJ mol^{-1});
ΔG^{I}_r	Variation of Gibbs' free energy at initial experiment condition (kJ mol^{-1}).

8 Competing Interests

The authors declare that they have no competing interests.

9 Authors' Contribution

All authors have planned the experiments. GM performed all the experiments, data treatment, statistics and mathematical modeling. GB treated and analysed all sequencing data. All authors have analysed and discussed the results. GM have written the paper. All authors have read, reviewed and approved the final manuscript. Experiments were conducted in Montréal branch of National Research Council of Canada from January to July of 2014.

10 Authors' Informations

GM is professor of sanitation and applied microbiology of the Agricultural Engineering College at Campinas State University (FEAGRI/UNICAMP). This research was developed as an invited researcher at National Research Council of Canada (NRC) from October/2013 to October/2014, under a post-doctoral program in biofuels in the São Carlos Engineering School at University of São Paulo (EESC/USP).

11 Acknowledgements

This work was supported by FAPESP – Fundação de Amparo a Pesquisa do Estado de São Paulo (processes 2010/18.463-9 and 2013/18.172-2 – G. Mockaitis and 2009/15.984-0 – M. Zaiat), and the NRC – National Research Council of Canada (project A1-004645 – S. Guiot).

The authors thankfully acknowledge Marie-Joseé Lévesque, Christine Maynard and Sylvie Sanschagrin for their assistance with the biomolecular techniques (DNA extraction, purification and PCR) and sequencing (through Ion Torrent™); and also Stephane Deschamps and Alain Corriveau for their valuable contribution with physicochemical analysis (HPLC and gas chromatography of alcohols).

12 References

1. Jones DT, Woods DR. Acetone-butanol fermentation revisited. Microbiol Rev. 1986;50:484–524.

2. Das D, Veziroglu T. Advances in biological hydrogen production processes. Int J Hydrogen Energy. Elsevier Ltd; 2008;33:6046–57.

3. Levin D. Biohydrogen production: prospects and limitations to practical application. Int J Hydrogen Energy. 2004;29:173–85.

4. Steinbusch KJJ, Hamelers HVM, Buisman CJN. Alcohol production through volatile fatty acids reduction with hydrogen as electron donor by mixed cultures. Water Res. 2008;42:4059–66.

5. Zverlov V V, Berezina O, Velikodvorskaya G a, Schwarz WH. Bacterial acetone and butanol production by industrial fermentation in the Soviet Union: use of hydrolyzed agricultural waste for biorefinery. Appl Microbiol Biotechnol. 2006;71:587–97.

6. Agler MT, Wrenn B a, Zinder SH, Angenent LT. Waste to bioproduct conversion with undefined mixed cultures: the carboxylate platform. Trends Biotechnol. Elsevier Ltd; 2011;29:70–8.

7. Dürre P. New insights and novel developments in clostridial acetone/butanol/isopropanol fermentation. Appl Microbiol Biotechnol. 1998;639–48.

8. Brynjarsdottir H, Wawiernia B, Orlygsson J. Ethanol Production from Sugars and Complex Biomass by Thermoanaerobacter AK 5□: The Effect of Electron-Scavenging Systems on End-Product Formation. Energy and fuels. 2012;26:4568–74.

9. Jessen JE, Orlygsson J. Production of ethanol from sugars and lignocellulosic biomass by Thermoanaerobacter J1 isolated from a hot spring in Iceland. J Biomed Biotechnol. 2012;2012:186982.

10. Georgieva TI, Ahring BK. Evaluation of continuous ethanol fermentation of dilute-acid corn stover hydrolysate using thermophilic anaerobic bacterium Thermoanaerobacter BG1L1. Appl Microbiol Biotechnol. 2007;77:61–8.

11. Li S, Lai C, Cai Y, Yang X, Yang S, Zhu M, et al. High efficiency hydrogen production from glucose/xylose by the ldh-deleted Thermoanaerobacterium strain. Bioresour Technol. Elsevier Ltd; 2010;101:8718–24.

12. Avci A, Dönmez S. Effect of zinc on ethanol production by two Thermoanaerobacter strains. Process Biochem. 2006;41:984–9.

13. Almarsdottir AR, Sigurbjornsdottir MA, Orlygsson J. Effect of various factors on ethanol yields from lignocellulosic biomass by Thermoanaerobacterium AK□□. Biotechnol Bioeng. 2012;109:686–94.

14. Koskinen PEP, Beck SR, Orlygsson J, Puhakka J a. Ethanol and hydrogen production by two thermophilic, anaerobic bacteria isolated from Icelandic geothermal areas. Biotechnol Bioeng. 2008;101:679–90.

15. Crespo CF, Badshah M, Alvarez MT, Mattiasson B. Ethanol production by continuous fermentation of D-(+)-cellobiose, D-(+)-xylose and sugarcane bagasse hydrolysate using the thermoanaerobe Caloramator boliviensis. Bioresour Technol. Elsevier Ltd; 2012;103:186–91.

16. Xu L, Tschirner U. Improved ethanol production from various carbohydrates through anaerobic thermophilic co-culture. Bioresour Technol. Elsevier Ltd; 2011;102:10065–71.

17. Mes-Hartree M, Saddler J. Butanol production of Clostridium acetobutylicum grown on sugars found in hemicellulose hydrolysates. Biotechnol Lett. 1982;4:247–52.

18. Maddox I. Production of ethanol and n-butanol from hexose/pentose mixtures using consecutive fermentations with Saccharomyces cerevisiae and Clostridium acetobutylicum. Biotechnol Lett. 1982;4:23–8.

19. Ounine K, Petitdemange H, Raval G, Gay R. Acetone-butanol production from pentoses by Clostridium acetobutylicum. Biotechnol Lett. 1983;5:605–10.

20. Li Z, Shi Z, Li X. Models construction for acetone-butanol-ethanol fermentations with acetate/butyrate consecutively feeding by graph theory. Bioresour Technol. Elsevier Ltd; 2014;159:320–6.

21. Kumar M, Goyal Y, Sarkar A, Gayen K. Comparative economic assessment of ABE fermentation based on cellulosic and non-cellulosic feedstocks. Appl Energy. Elsevier Ltd; 2012;93:193–204.

22. Nimcevic D, Gapes JR. The acetone-butanol fermentation in pilot plant and pre-industrial scale. J Mol Microbiol Biotechnol. 2000;2:15–20.

23. Kleerebezem R, van Loosdrecht MCM. Mixed culture biotechnology for bioenergy production. Curr Opin Biotechnol. 2007;18:207–12.

24. Puig S, Coma M, Monclús H, van Loosdrecht MCM, Colprim J, Balaguer MD. Selection between alcohols and volatile fatty acids as external carbon sources for EBPR. Water Res. 2008;42:557–66.

25. Mohan SV, Babu VL, Sarma PN. Effect of various pretreatment methods on anaerobic mixed microflora to enhance biohydrogen production utilizing dairy wastewater as substrate. 2008;99:59–67.

26. O-Thong S, Prasertsan P, Birkeland N-K. Evaluation of methods for preparing hydrogen-producing seed inocula under thermophilic condition by process performance and microbial community analysis. Bioresour Technol. Elsevier Ltd; 2009;100:909–18.

27. Pendyala B, Chaganti SR, Lalman J a., Shanmugam SR, Heath DD, Lau PCK. Pretreating mixed anaerobic communities from different sources: Correlating the hydrogen yield with hydrogenase activity and microbial diversity. Int J Hydrogen Energy. Elsevier Ltd; 2012;37:12175–86.

28. Luo G, Xie L, Zou Z, Wang W, Zhou Q. Evaluation of pretreatment methods on mixed inoculum for both batch and continuous thermophilic biohydrogen production from cassava stillage. Bioresour Technol. Elsevier Ltd; 2010;101:959–64.

29. Luo G, Karakashev D, Xie L, Zhou Q, Angelidaki I. Long-term effect of inoculum pretreatment on fermentative hydrogen production by repeated batch cultivations: homoacetogenesis and methanogenesis as competitors to hydrogen production. Biotechnol Bioeng. 2011;108:1816–27.

30. Cheong D-Y, Hansen CL. Bacterial stress enrichment enhances anaerobic hydrogen production in cattle manure sludge. Appl Microbiol Biotechnol. 2006;72:635–43.

31. Mu Y, Yu H-Q, Wang G. Evaluation of three methods for enriching H2-producing cultures from anaerobic sludge. Enzyme Microb Technol. 2007;40:947–53.

32. Zhu H, Beland M. Evaluation of alternative methods of preparing hydrogen producing seeds from digested wastewater sludge. Int J Hydrogen Energy. 2006;31:1980–8.

33. Wang J, Wan W. Comparison of different pretreatment methods for enriching hydrogen-producing bacteria from digested sludge. Int J Hydrogen Energy. 2008;33:2934–41.

34. Hu B, Chen S. Pretreatment of methanogenic granules for immobilized hydrogen fermentation. Int J Hydrogen Energy. 2007;32:3266–73.

35. Ren N, Guo W, Wang X, Xiang W, Liu B, Ding J, et al. Effects of different pretreatment methods on fermentation types and dominant bacteria for hydrogen production. Int J Hydrogen Energy. 2008;33:4318–24.

36. Kumar M, Gayen K, Saini S. Role of extracellular cues to trigger the metabolic phase shifting from acidogenesis to solventogenesis in Clostridium acetobutylicum. Bioresour Technol. Elsevier Ltd; 2013;138:55–62.

37. Angelidaki I, Petersen SP, Ahring BK. Applied Microbiolog . v Effects of lipids on thermophilic anaerobic digestion and reduction of lipid inhibition upon addition of bentonite. 1990;469–72.

38. Sander R. Compilation of Henry ' s Law Constants for Inorganic and Organic Species of Potential Importance in Environmental Chemistry. 1999.

39. Lide DR, Frederikse HPR, editors. CRC Handbook of Chemistry and Physics. 76th ed. Boca Ratón, FL, USA: CRC Press Inc.; 1995.

40. APHA. Standard methods for the examination of water and wastewater. 21st ed. Washington DC; 2005.

41. Dilallo R, Albertson O. Volatile Acids by Direct Titration. J Water Pollut Control Fed. 1961;33:356–65.

42. Ripley L, Boyle W, Convrese J. Improved alkalimetric monitoring for anaerobic digestion of high-strength wastes. J Water Pollut Control Fed. 1986;58:406–11.

43. Guiot SR, Cimpoia R, Carayon G. Potential of wastewater-treating anaerobic granules for biomethanation of synthesis gas. Environ Sci Technol. 2011;45:2006–12.

44. Muyzer G, Dewaal EC, Uitterlinden AG. Profiling of complex microbial populations by desnaturing gradient gel electrophoresis analysis ofpolymerase chain reaction amplified genes coding for 16S ribosomal RNA. Appl Environ Microbiol. 1993;59:695–700.

45. Griffiths RI, Whiteley a S, O'Donnell a G, Bailey MJ. Rapid method for coextraction of DNA and RNA from natural environments for analysis of ribosomal DNA- and rRNA-based microbial community composition. Appl Environ Microbiol. 2000;66:5488–91.

46. Lévesque MJ, La Boissière S, Thomas JC, Beaudet R, Villemur R. Rapid method for detecting Desulfitobacterium frappieri strain PCP-1 in soil by the polymerase chain reaction. Appl Microbiol Biotechnol. 1997;47:719–25.

47. Berthelet M, Whyte LG, Greer CW. Rapid, direct extraction of DNA from soils for PCR analysis using polyvinylpolypyrrolidone spin columns. FEMS Microbiol Lett. 1996;138:17–22.

48. Wang Q, Garrity GM, Tiedje JM, Cole JR. Naive Bayesian classifier for rapid assignment of rRNA sequences into the new bacterial taxonomy. Appl Environ Microbiol. 2007;73:5261–7.

49. Claesson MJ, O'Sullivan O, Wang Q, Nikkilä J, Marchesi JR, Smidt H, et al. Comparative analysis of pyrosequencing and a phylogenetic microarray for exploring microbial community structures in the human distal intestine. PLoS One. 2009;4:e6669.

50. Mavrovouniotis ML. Group contributions for estimating standard gibbs energies of formation of biochemical compounds in aqueous solution. Biotechnol Bioeng. 1990;36:1070–82.

51. Mavrovouniotis ML. Errata Group Contributions for Estimating Standard Gibbs Energies of Formation of Biochemical Compounds in Aqueous Solution. 1991;38:803–4.

52. Harper SR, Pohland FG. Recent Developments in Hydrogen Management During Anaerobic Biological Wastewater Treatment. Biotechnol Bioeng. 1985;28:585–602.

53. Speece RE. Anaerobic biotechnology for industrial wastewater. Press A, editor. Vanderbilt University; 1996.

54. Caspi R, Altman T, Dale JM, Dreher K, Fulcher CA, Gilham F, et al. The MetaCyc database of

metabolic pathways and enzymes and the BioCyc collection of pathway/genome databases. Nucleic Acids Res. 2010;38:D473-9.

55. Leifson E, Hugh R. A new type of polar monotrichous flagellation. J Gen Microbiol. 1954;10:68–70.

56. Tracy BP, Jones SW, Fast AG, Indurthi DC, Papoutsakis ET. Clostridia: the importance of their exceptional substrate and metabolite diversity for biofuel and biorefinery applications. Curr Opin Biotechnol. 2012;23:364–81.

57. Ueki A, Hirono T, Sato E, Mitani A, Ueki K. Ethanol and amylase production by a newly isolated Clostridium sp. World J Microbiol …. 1991;7:385–93.

58. Bruant G, Lévesque M-J, Peter C, Guiot SR, Masson L. Genomic analysis of carbon monoxide utilization and butanol production by Clostridium carboxidivorans strain P7. PLoS One. 2010;5:e13033.

13 One-Sentence Summary

The inoculum pretreatment acid and thermal improved significantly the production of both ethanol and butanol, through an anaerobic solventogenic process, using acetate and butyrate as carbon source and H_2 as electron donor.

14 Supplementary Information

14.1 Modified Boltzmann Sigmoidal Equation

This addendum has the objective to explain all the steps to achieve the modified Boltzmann sigmoidal equation as presented in Equation 1. In addition to this, all the assumption to infer the starting and ending points of the exponential growth phase, shown by Equations 2 and 3 will be explained as well.

The sigmoidal is the standard shape of a bacterial monophasic growth curve. For applying such model, it was assumed that microbial growth could be linearly associated with both substrates consumption and products production time profiles. Thus, the sigmoidal function was chosen to describe the time

profile of ethanol and butanol production, and it was modified so its parameters could mean a biological significance.

The original form of sigmoidal equation proposed by Boltzmann in 1879 is a logistic function modification, and is shown by Equation A.

Equation A

Where is the maximum value reached by the ordinate, defined by ; is the minimum value reached by the ordinate, defined by ; is the abscissa value when the slope value is maximum, defined by ; and is an slope correlated value which describes its behavior.

For applying this mathematical model for describing more adequately the behavior of a microbiological system, it was considered some boundary conditions. Since this model was applied for alcohol production evaluation, and none of these products was detected at the beginning of the experiments (when time = 0), the parameter was considered null (i.e.). Also, in spite of the value of the parameter could be related with the slope of the sigmoidal function, it does not represent any kind of comparable parameter. In this sense, this parameter was replaced by the value of the maximum slope of the sigmoidal function, determined as shown by Equation B.

Equation B

The maximum value of the function slope is reached when , which simplifies the Equation B into the Equation C.

Equation C

Replacing the Equation C in the Equation A, also constraining the value as boundary condition, it is possible to rewrite the Equation A in terms of , as depicted in Equation D, which is the modified Boltzmann equation described as Equation 1.

Equation D

The Figure A shows the Equation D and its derivative for arbitrary parameters values, and places the parameters in the graph.

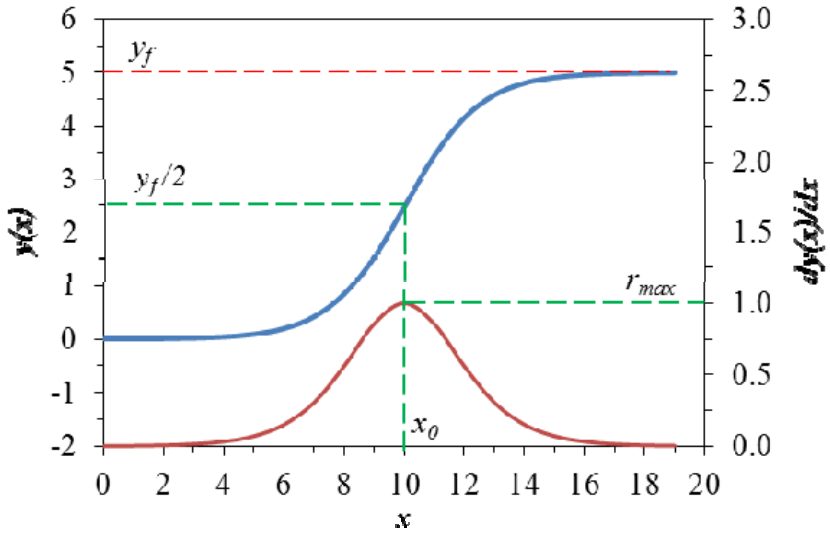

Figure A – Shape of the modified Boltzmann equation (blue filled line,) and its derivative (red filled line,)), for ; and . The dashed red line shows the value of , as the dashed green line shows in and for .

Throughout this modified equation, it was possible to determine, only by evaluating its parameters, the maximum production of ethanol and butanol (), its maximum rate () and the time in which this maximum rate was achieved ().

The initial and final points of the exponential phase (and) are also important parameters to compare and evaluate the process. These values were estimated approximating the shape of the exponential phase to a straight-line equation, in which the parameter was the angular coefficient. Thus, the behavior of in between the interval [] was modeled as a function , described by the Equation E, only for means to calculate both and .

Equation E

Thus, the parameters and are calculated equating the Equation E to 0 and , respectively, leading then to the expressions represented for the Equations F and G.

Equation F

Equation G

These parameters shall be considered as an estimation of the initial and final time of the exponential growth phase. A graphic explanation of this method is depicted on Figure B.

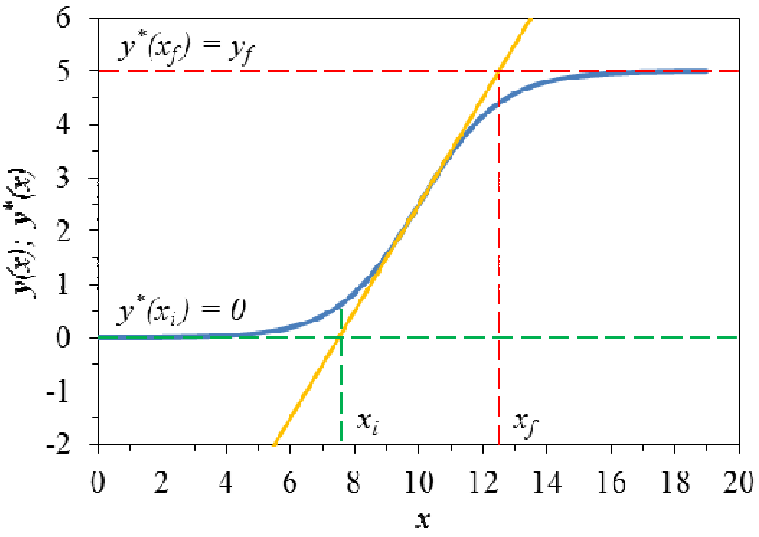

Figure B – Estimation of initial () and final () time of the exponential growth phase. The Equation E function (yellow filled line, and the modified Boltzmann equation (blue filled line,) are shown. The green and the red dashed lines show the boundary condition for calculation of and , respectively.

Finally, the time length of the exponential time could be obtained subtracting from , leading to the

Equation H.

Equation H